

# Jet quenching and neutral pion production in Au+Au collisions at RHIC

A. K. Chaudhuri\*

Variable Energy Cyclotron Centre  
1-AF, Bidhan Nagar, Kolkata - 700 064

In the jet quenching model, we have analysed the PHENIX data on nuclear modification factor of  $\pi^0$ , in Au+Au collisions at  $\sqrt{s}=200$  GeV, and extracted the initial gluon density of the medium produced. In jet quenching, partons lose energy in the medium, depending on the medium density as well as on the in-medium path length. Systematic analysis indicate that in most central (0-10% centrality) collisions, medium density is very large  $dN_g/dy \sim 2150$ . Medium density decreases exponentially as the collision centrality decreases and in very peripheral (70-92% centrality) collisions,  $dN_g/dy \sim 3$ . Initial energy density of the medium also decreases smoothly from  $\varepsilon_0 \sim 20$  GeV/fm<sup>3</sup> in most central collisions to  $\varepsilon_0 \sim 3$  GeV/fm<sup>3</sup> in most peripheral collisions. Very large  $dN_g/dy$  or  $\varepsilon_0$  indicate very dense matter formation in central Au+Au collisions.

## I. INTRODUCTION

One of the predictions of quantum chromodynamics is the possible existence of a deconfined state of quarks and gluons. In relativistic heavy ion collisions, under certain conditions (sufficiently high energy density and temperature) ordinary hadronic matter (where quarks and gluons are confined) can undergo a phase transition to a deconfined matter, commonly known as quark gluon plasma (QGP). Over the years, nuclear physicists are trying to produce and detect this new phase of matter, first at CERN SPS and now at Relativistic Heavy Ion Collider (RHIC). At RHIC several new results are obtained, most important among them is the high  $p_T$  suppression in Au+Au collisions and its absence in d+Au collisions. All the four experiments, STAR, PHENIX, PHOBOS and BRAHMS [1–4] observed that high  $p_T$  hadron production in Au+Au collisions at  $\sqrt{s} = 200$  GeV (as well as at  $\sqrt{s} = 130$  GeV), *scaled* by the average number of binary collisions, is suppressed with respect to pp collisions. The suppression is more in central collisions than in peripheral collisions. The observation has created an excitement in nuclear physics community, as a possible signature, if not of QGP, of creation of highly dense matter in central Au+Au collisions.

One of the explanations offered for the high  $p_T$  suppression at RHIC is the jet quenching [5,6]. In the fragmentation picture [7], the single parton spectrum is convoluted with the probability for a parton  $i$  to hadronize into a hadron  $h$ , which carries a fraction  $z < 1$  of the momentum of the parent parton. Unlike in pp collisions, in AA collisions, partons produced in the initial hard scattering has to propagate through a medium before fragmentation. While propagating through the medium, the partons can suffer energy loss through multiple scattering. As a result, at the time of fragmentation to hadrons, the partons will have less energy and consequently will produce less hadrons than would have otherwise. Several authors have studied high  $p_T$  production at RHIC energy in Au+Au collisions [8–15]. The LO or NLO pQCD models with jet quenching can well explain the high  $p_T$  suppression, implying large parton energy loss or high initial gluon density. In [8] gluon density, at an initial time  $\tau_0 = 0.2$  fm was estimated to be 15-30 times higher than that in a normal nuclear matter.

Apart from the jet quenching, alternative explanations are also offered for the high  $p_T$  suppression. Indeed, leading hadrons from the jet fragmentation can possibly have strong interactions with the medium created and possibly be absorbed or its  $p_T$  be shifted to lower values leading to the high  $p_T$  suppression. In [16] high  $p_T$  suppression, due to final state hadronic interactions, was considered. It was argued that partons cannot materialize into hadrons in a deconfined phase. Fragmentation can occur only outside the deconfined phase or in vacuum. It was argued that high  $p_T$  (pre-)hadrons can well be realized inside the late stage of the fireball. Then interaction of the (pre-)hadrons with bulk hadronic matter could lead to the observed suppression. RHIC data on high  $p_T$  suppression can be partially explained in the model. Final state hadronic interaction was also used by Capella et al [17] to explain the high  $p_T$  suppression. In their model, high  $p_T$  hadrons interact with the comovers and their  $p_T$  is shifted to smaller values. Due to steepness of the  $p_T$  distribution the effect could be large. Indeed, it was shown that the RHIC data are well explained in such a model [17]. Recently Xin-Nian [14] has argued strongly against models using the final state hadronic interaction to explain RHIC high  $p_T$  suppression. He argued that hadron formation time could not be small, rather large, in the range of 30-40 fm, much larger than the typical medium size or lifetime of the dense medium. Moreover, nearly flat  $p_T$  dependence of the observed suppression at high  $p_T$  empirically leads to a linear energy dependence of the hadronic energy loss. Since the hadron formation time is proportional to hadron or jet energy, the

total energy loss due to hadron rescattering or absorption decreases with energy. He argued that observed high  $p_T$  suppression at RHIC could only be due to partonic energy loss.

In the present paper, a systematic analysis of PHENIX data on  $\pi^0$  suppression is presented. Data are analysed in the jet quenching model. In jet quenching, partons suffer energy loss in the medium produced in Au+Au collisions. Partonic energy loss depend on the in-medium path length and on the initial gluon density [5]. For a reliable estimate of the gluon density, in-medium path length should be accurate. In the present work, in-medium path length, in each centrality ranges of collisions, is estimated in the Glauber model. Initial gluon density in different centrality ranges of collisions are the extracted from a fit to the PHENIX  $\pi^0$  data on the nuclear modification factor. With a single parameter, the gluon density, large  $p_T > 4\text{GeV}$  part of the PHENIX data are well explained. Our analysis indicate very large initial gluon density,  $dN_g/dy \sim 2158$  in 0-10% centrality collisions. Corresponding energy density  $\varepsilon_0 \sim 20\text{GeV}/fm^3$ . Gluon density decreases exponentially from central to peripheral collisions and in very peripheral (70-92% centrality) collisions. it is very small,  $dN_g/dy \sim 3$ .

The plan of the paper is as follows: In section 2, we have described the pQCD model for hadron production. In section 3, results of our analysis of PHENIX data are presented. Summary and conclusions are given in section 4.

## II. PQCD MODEL FOR HADRON PRODUCTION

Details of high  $p_T$  hadron production in pp collisions could be found in [18]. In a pQCD model, the differential cross section for production of a hadron  $h$  with transverse momentum  $q_T$ , at rapidity  $y$ , in pp collisions can be written as ,

$$\frac{d\sigma^{pp \rightarrow hX}}{dq_T^2 dy} = K J(m_T, y) \int \frac{dz}{z^2} \int dy_2 \sum_{\langle ij \rangle, \langle kl \rangle} \frac{1}{1 + \delta_{kl}} \frac{1}{1 + \delta_{ij}} \quad (1)$$

$$\left\{ x_1 f_{i/A}(x_1, Q^2) x_2 f_{j/B}(x_2, Q^2) \left[ \frac{d\hat{\sigma}^{ij \rightarrow kl}}{d\hat{t}}(\hat{s}, \hat{t}, \hat{u}) D_{k \rightarrow h}(z, \mu^2) + \frac{d\hat{\sigma}^{ij \rightarrow kl}}{d\hat{t}}(\hat{s}, \hat{u}, \hat{t}) D_{l \rightarrow h}(z, \mu^2) \right] \right.$$

$$\left. + x_1 f_{j/A}(x_1, Q^2) x_2 f_{i/B}(x_2, Q^2) \left[ \frac{d\hat{\sigma}^{ij \rightarrow kl}}{d\hat{t}}(\hat{s}, \hat{u}, \hat{t}) D_{k \rightarrow h}(z, \mu^2) \frac{d\hat{\sigma}^{ij \rightarrow kl}}{d\hat{t}}(\hat{s}, \hat{t}, \hat{u}) D_{l \rightarrow h}(z, \mu^2) \right] \right\}$$

Details of the equation can be found in [18]. Here, the parameter  $K$  takes into account the higher order corrections. For the partonic collisions  $ij \rightarrow kl$ ,  $x_1$  and  $x_2$  are the fractional momentum of the colliding partons  $i$  and  $j$ ,  $x_{1,2} = \frac{p_T}{\sqrt{s}}(e^{\pm y_1} + e^{\pm y_2})$ ,  $y_1$  and  $y_2$  being the rapidities of the two final state partons  $k$  and  $l$ . For the parton distribution,  $f(x, Q^2)$ , we have used the CTEQ5L parton distribution, with the factorization scale  $Q^2 \approx p_T^2$ . In Eq.1,  $d\hat{\sigma}^{ab \rightarrow cd}/d\hat{t}$  is the sub process Cross-section. Only 8 sub processes contribute, they are listed in [19].  $D_h(z, \mu^2)$  is the fragmentation function for the final state partons. We have used KPP parameterization [20] with fragmentation scale  $\mu^2 \approx q_T^2$ . The integration region for  $y_2$ ,  $-\ln(\sqrt{s}/p_T - e^{-y_f}) < y_2 < \ln(\sqrt{s}/p_T - e^{y_f})$ , is over the whole phase space, whereas that for  $z$  is

$$\frac{2m_T}{\sqrt{s}} \cosh y \leq z \leq \min[1, \frac{q_T}{p_0} J(m_T, y)] \quad (2)$$

with,  $J(m_T, y) = (1 - \frac{m^2}{m_T^2 \cosh y})^{-1}$ .  $p_0$  is the cut off used to regulate infrared singularity. It is a parameter and in the present work we have used  $p_0=1.0$  GeV.

In Fig.1, we have shown the fit obtained to the PHENIX pp data on  $\pi^0$  production with  $K=1.29 \pm 0.02$ . LO pQCD model give reasonably good description of the high  $p_T$   $\pi^0$  production in pp collisions at RHIC energy. We note that better description could be obtained with generalized parton distribution [21], however, at the expense of an additional parameter.

Following the standard procedure,  $p_T$  distribution of neutral pions in Au+Au collisions could be obtained as,

$$\frac{d\sigma^{AA \rightarrow hX}}{d^2 q_T dy} = \int_{b_{min}}^{b_{max}} d^2 b d^2 s T_A(\mathbf{b} - \mathbf{s}) T_B(\mathbf{s}) \frac{d\sigma^{NN \rightarrow hX}}{d^2 q_T dy} \quad (3)$$

The impact parameter integration ranges ( $b_{min}$  and  $b_{max}$ ) are chosen according to centrality of collisions. They are listed in table 1. In this picture, all the nuclear information is contained in the thickness function,  $T_A(\mathbf{b}) = \int \rho(\mathbf{b}, z) dz$ . We have used Woods-Saxon form for the density  $\rho(r)$ ,

$$\rho(r) = \frac{\rho_0}{1 + e^{(r-R)/a}} \quad (4)$$

For Au,  $R = 6.38 fm$  and  $a = 0.535 fm$ . The central density  $\rho_0$  is obtained from the normalizing condition,  $\int \rho(r) d^3r = A$ .

In AA collisions, vacuum parton distribution ( $f(x, q^2)$ ) as well as the fragmentation function ( $D_h(z, \mu^2)$ ) will be modified. It is well known that parton distribution in bound nucleon differ from that of a free nucleon (the EMC effect). We take care of it using HIJING parameterization. However, its effect on high  $p_T$  suppression is small. Medium modification of fragmentation function is not very clear. Ideally, one should solve the DGLAP evolution equation for fragmentation functions, taking into account the medium effects on the splitting function. Such an analysis has not been performed. In the jet quenching or energy loss model, high energy partons loses a fraction  $\varepsilon$  of its energy while passing through the medium and then fragments in the vacuum with the normal vacuum fragmentation function with the corresponding shifted momentum fraction. Any modification of virtuality dependence of the fragmentation function is neglected. The medium modified fragmentation function is then written as,

$$D_{i \rightarrow h}^{med}(z, \mu^2) \rightarrow \int d\varepsilon p(\varepsilon) \frac{1}{1-\varepsilon} D_{i \rightarrow h}\left(\frac{z}{1-\varepsilon}, \mu^2\right) \quad (5)$$

where  $p(\varepsilon)$  is the probability that prior to hadronisation, a parton with energy  $E$  loss  $\varepsilon E$  energy in the medium. In the Poisson approximation of independent gluon emission, probability distribution of fractional energy loss  $p(\varepsilon)$  can be obtained iteratively from single inclusive gluon radiation spectrum  $dN/dx$ . In the present paper, we however choose a simpler Delta distribution,  $p(\varepsilon) = \delta(\varepsilon)$ . Delta function produces a much stronger effect due to rapid  $z$  dependence of the fragmentation function. With delta function for  $p(\varepsilon)$ , implementation of energy loss is simple. For  $\Delta E$  loss of energy, the fragmentation function in the elemental cross section, is changed as,

$$z D_h(z) = z^* D_h(z^*), \quad z^* = z/(1 - \Delta E/E) \quad (6)$$

As the fragmentation functions are peaked at low  $z$ , partonic energy loss will necessarily lead to less number of hadron production.

At RHIC, nuclear effects on the inclusive spectra, in different centrality ranges of collisions, were measured in terms of the nuclear modification factor ( $R_{AA}$ ). It is defined as,

$$R_{AA} = \frac{d^2 N/dp_T dy (Au + Au)}{T_{AA} d^2 \sigma/dp_T dy (pp)} \quad (7)$$

where  $T_{AA} = \langle N_{bin} \rangle / \sigma_{inel}$  from a Glauber calculation accounts for the nuclear collision geometry. The nuclear modification factor will be unity, had there been no nuclear effects on high  $p_T$  production. In Fig.2, PHENIX data on nuclear modification factor for neutral pions, in different centrality ranges of collisions are shown. PHENIX data show considerable nuclear effects ( $R_{AA} < 1$ ) in central collisions.

### III. PARTONIC ENERGY LOSS

In the jet-quenching picture, hadronic spectra are determined by the energy loss of partons. Partonic energy loss in a medium is a complex phenomena. Recently, much progress has been made in understanding partonic energy loss [22–28]. Partons lose energy mainly due to gluon radiation. QCD radiative energy loss in a finite size QGP was solved analytically in [23]. In the leading log approximation, BDMS [23] prediction is ,

$$\Delta E_{BDMS} = \frac{C_F \alpha_s}{4} \frac{L^2 \mu_D^2}{\lambda_g} \tilde{v} \quad (8)$$

where  $L$  is the length of the plasma,  $\mu_D$  is the Debye screening mass,  $\lambda_g$  is the mean free path of the gluons in QGP,  $C_F$  is the color Casimir for the partons ( $C_F=3$  for gluons and  $4/3$  for quarks) and the factor  $\tilde{v}$  grows smoothly with  $L$ , at  $L \gg \lambda_g$ ,  $\tilde{v} \approx \log(L/\lambda_g)$ .

BDMS energy loss is independent of parton energy. Recently, Gyulassy, Levai and Vitev (GLV) [25], calculated the partonic energy loss in the light-cone path integral approach. GLV form of the partonic energy loss depends logarithmically on the parton energy. Discrepancy between the energy dependence of the radiative energy losses in two approaches is understood to be due to leading log approximation in BDMS approach [29].

Gluon radiation from a static source has a characteristic quadratic dependence on the in-medium path length ( $L$ ) Eq.8. The path dependence is changed if the medium is expanding. For example, in an one dimensionally expanding medium, the quadratic dependence is diluted to a linear dependence [25]. Under certain approximations, analytic expression for partonic energy loss, in a medium undergoing Bjorken expansion , was obtained by Gylusaay et al [25].

$$\Delta E = \frac{9C_F\pi\alpha_s^3}{4} \frac{1}{A_T} \frac{dN_g}{dy} L \ln\left(\frac{2E}{\mu_D^2 L} + \frac{3}{\pi}\right) \quad (9)$$

where as before  $L$  is the in-medium path length and  $A_T$  is the transverse area. It can be seen that transverse gluon density  $\frac{1}{A_T} \frac{dN_g}{dy}$  as well as the medium path length controls the partonic energy loss.

In addition to gluonic radiation, partons suffer collisional energy loss. There are marked differences between radiative and collisional energy loss. Detailed calculation of collisional energy loss of partons has not been made.  $\Delta E_{coll}$  is independent of in-medium path length and depend logarithmically on energy. It is determined mainly by the medium temperature [30],

$$\frac{dE_{coll}}{dz} \propto \alpha_s^2 T^2 \ln E/T \quad (10)$$

In general radiative energy loss dominate over collisional energy loss. However, for high  $p_T > 10\text{GeV}$  partons, collisional energy loss can be substantial (30-40%) [31]. Since PHENIX  $\pi^0$  data are limited to  $p_T < 10\text{GeV}$ , we have neglected the collisional energy loss.

#### IV. RESULTS

PHENIX collaboration measured nuclear modification factor ( $R_{AA}$ ) for  $\pi^0$ , in several centrality ranges of collisions. In table 1, we have listed the centrality ranges of collisions analysed in the present paper along with the corresponding impact parameter ranges ( $b_{min}$  and  $b_{max}$ ). For completeness purpose, we have also listed the Glauber model calculation of average number of binary collisions and number of participants in those centrality ranges of collisions. In the jet quenching model, particle spectra depend on the energy loss suffered by the partons. In the GLV form, energy loss depend on (see Eq.9), (i) the initial transverse gluon density (ii) the Debye screening mass and (iii) the in-medium path length. We have assumed that in a centrality range of collisions, partons travel an average distance  $L$  and suffer energy loss in a medium with average initial transverse gluon density  $\rho^{trans} = \frac{1}{A_T} \frac{dN_g}{dy}$ . Since energy loss depend on the product  $L\rho^{trans}$ , accurate determination of the density of the medium requires accurate in-medium path length. We have calculated the average in-medium path length in a Glauber model (see appendix). In-medium path length  $L$  in different centrality ranges of collisions are listed in table 1. In 0-10% central collisions, the average medium path length is 5.17 fm. It is nearly a factor of 1.5 times smaller than the length  $4/3R_A$ , used by Vitev et al [13] in their calculation. In-medium path length reduces by a factor of 5 in very peripheral collisions. For the screening mass  $\mu_D$  we use a fixed value  $\mu_D=0.8$  GeV. This specific value was obtained from a fit to PHENIX 0-10% centrality  $\pi^0$  data, with both the gluon density and  $\mu_D$  as free parameters.

With  $\rho^{trans}$  as the only free parameter, nuclear modification factors for  $\pi^0$  are fitted, using the MINUIT minimization programme. pQCD is applicable only for high  $p_T$ . Consequently only a part of the data,  $p_T > 4\text{GeV}$  are considered for the fitting. In Fig.2, PHENIX data along with the fit obtained are shown. Within the error bars, high  $p_T$  part of the PHENIX data on the nuclear modification factor are well described. Energy loss or jet quenching can explain the dramatic variation of nuclear effects, in  $\pi^0$  production, in terms of a single parameter, the average transverse gluon density  $\rho^{trans}$ . However, we note the discrepancy in the  $p_T$  dependence of the experimental  $R_{AA}$  and the pQCD predictions. At large  $p_T$ , within the error bars, experimental  $R_{AA}$  donot show any  $p_T$  dependence. The pQCD model predictions, on the other hand show  $p_T$  dependence, suppression decreasing with  $p_T$ . In the jet quenching models, relative energy loss ( $\Delta E/E$ ) is the relevant quantity. In GLV form of partonic energy loss,  $\Delta E/E \propto \ln E/E$ . As a results, at large  $p_T$ , partons lose less energy and suppression is reduced. PHENIX data have large error bars, reflective of poor statistics at RHIC. Good statistic data in extended  $p_T$  range can resolve the issue, whether or not high  $p_T$  suppression is  $p_T$  independent and test the GLV form of partonic energy loss.

Initial transverse gluon density ( $\rho^{trans}$ ) in different centrality ranges of collisions, as extracted from the PHENIX data, are listed in table 1. In 0-10% centrality Au+Au collisions, gluon density is very large,  $\rho_{0-10\%}^{trans} \geq 21.08 \pm 1.00$ . Density decreases as the centrality of the collisions decreases. In very peripheral collisions,  $\rho_{70-92\%}^{trans} = 4.5 \pm 1.22$ , nearly a factor of 5 less than density in very central collisions. In Fig.3, we have shown the extracted initial transverse gluon density, as a function of the number of participants. The linear relation,

$$\frac{1}{A_T} \frac{dN_g}{dy} = 3.74 + 0.11 \frac{N_{part}}{2}, \quad (11)$$

describe the extracted initial transverse gluon density in different centrality ranges of collisions.

Initial rapidity density of gluons ( $dN_g/dy$ ) can also be estimated. The average transverse area ( $A_T$ ), in each centrality ranges of collisions, is easily calculated. At an impact parameter  $b$ , the transverse area is elliptical and

$A_T = \pi ab$  with  $a = \sqrt{R^2 - b^2/4}$  and  $b = R - b/2$ . We calculate the average transverse area taking the simple average of  $A_T$  at two limits of the impact parameter ( $b_{min}$  and  $b_{max}$ ) ranges. In table 1, average transverse area  $A_T$  in different centrality ranges of collisions are listed.  $A_T$  decreases very rapidly as the collision centrality decreases. While in very central collisions,  $A_T \sim 100 fm^{-2}$ , in very peripheral collisions,  $A_T < 1 fm^{-2}$ . This is reflected in gluon rapidity density  $\frac{dN_g}{dy}$  (see table 1). Gluon density decreases exponentially with centrality. In 0-10% centrality collisions, initial gluon density,  $\frac{dN_g}{dy} \sim 2158$ , and in very peripheral collisions  $dN_g/dy \sim 3$ . Gluon density in 0-10% centrality collisions, is nearly factor of 2 larger than the density obtained by Vitev et al [26]. In 0-10% central collisions, they obtained,  $dN_g/dy \sim 1000-1200$ . The difference is mainly due to difference in the estimate of average medium path length. Average medium path length ( $\langle L \rangle = 4/3R_A$ ) used in [13] is nearly a factor of 1.5 larger than the Glauber model estimate used presently.

In Fig.4, we have shown the initial rapidity density of gluons as a function of the average path length  $\langle L \rangle$  in the medium. Gluon density increases exponentially with the medium path length ( $L$ ) and are well described by the empirical relation,

$$\frac{dN_g}{dy} = A \exp(\mu L) \quad (12)$$

with  $A = 0.2$  and  $\mu = 1.8 fm^{-1}$ . Exponential dependence of initial gluon density on medium path length is very interesting. It is indicative of exponential loss of gluon intensity in a medium,  $I = I_0 \exp(-\mu L)$ .

We have also estimated the initial energy density in each centrality ranges of collisions. If  $\langle p \rangle$  is the mean transverse momentum of gluons, energy density is,

$$\varepsilon_0 \approx \frac{\langle p \rangle^2}{A_T} \frac{dN_g}{dy} \quad (13)$$

At RHIC, mean transverse momentum is  $\langle p_T \rangle \sim 0.4 - 0.5$  GeV. Assuming duality between particles and gluons,  $\langle p \rangle = \langle p_T \rangle_{particle}$ , the initial transverse gluon density is easily converted into initial energy density. They are shown in Fig.5 as a function of participant number. In most central collisions, energy density as high as  $20 GeV/fm^3$ . The value agree reasonably well with X.N. Wang's estimate that in central Au+Au collisions, compared to cold nuclear matter ( $\varepsilon_{cold} \sim 0.16 GeV/fm^3$ ), 100 times larger energy density is produced. As the collision centrality decreases, energy density decreases linearly and in very peripheral collisions  $\varepsilon_0 \approx 4 GeV/fm^3$ . The empirical relation,

$$\varepsilon(N_{part}) = 3.84 + 0.11 \frac{N_{part}}{2} (GeV/fm^3), \quad (14)$$

well describe the energy density as a function of number of participants. We note that even in peripheral collisions, the deduced energy density is very large compared to cold nuclear matter ( $\varepsilon_{cold} \sim 0.16 GeV/fm^3$ ). Indeed, it is larger than the critical energy density for QGP phase transition is  $\sim 1 GeV/fm^3$ .

It is interesting to see the model prediction at LHC energy. At LHC, centre of mass energy is very large ( $\sqrt{s}=1.148$  TeV). High  $p_T$  particles will be more abundant and  $R_{AA}$  could be measured more accurately in extended  $p_T$  range. In Fig.6, we have shown the predicted nuclear modification factor ( $R_{AA}$ ) in 0-10% centrality Au+Au collisions at LHC energy, for an initial transverse gluon density,  $\frac{1}{A_T} \frac{dN_g}{dy} = 20$ . Between  $p_T=5$  to 20 GeV, suppression is reduced by more than a factor of two. For comparison,  $R_{AA}$  at RHIC energy is also shown (the red line). Interestingly, for a fixed gluon density, suppression is more at RHIC than at LHC. We also note that whether or not GLV form of partonic energy loss give correct  $p_T$  dependence can be verified at LHC if  $R_{AA}$  is measured accurately in the  $p_T$  range, 5-20 GeV.

In Fig.7, we have shown the predicted nuclear modification factor ( $R_{AA}$ ), at a fixed  $p_T=5$  GeV, as a function of the initial transverse gluon density, in 0-10% centrality collisions. Both at RHIC and LHC energy, as expected,  $R_{AA}$  decreases with increasing gluon density. However, here again, we find that suppression is less at LHC energy than at RHIC energy. At LHC, 30% larger gluon density is required to obtain suppression similar to RHIC energy ( $R_{AA} \sim 0.2$ ).

## V. SUMMARY AND CONCLUSIONS

To summarise, we have presented a systematic analysis of the PHENIX data, on the nuclear modification factor for  $\pi^0$ 's, in Au+Au collisions, at  $\sqrt{s}=200$  GeV. Data are analysed in the Jet-quenching model, with the GLV form for the partonic energy loss in an one dimensionally expanding medium. GLV form of Partonic energy loss depend

on the medium path length and initial (transverse) gluon density. Medium path lengths in different centrality ranges of collisions are calculated in a Glauber model and initial (transverse) gluon densities are extracted from a fit to the data. From central to peripheral collisions, initial gluon density decreases exponentially. In 0-10% centrality collisions, present analysis give,  $dN_g/dy \sim 2158$ , nearly a factor of 2 larger than the value obtained by Vitev et al [26]. The difference is mainly due to different estimate of in-medium path length. We also find that the extracted gluon densities follow the empirical relation  $dN_g/dy = 0.2exp(1.8L)$ ,  $L$  being the in-medium path length. The result is interesting. Like photons, gluon intensity is exponentially attenuated in the medium, with attenuation coefficient  $\mu = 1.8fm^{-1}$ . Assuming gluon-hadron duality, we have also estimated initial energy density ( $\varepsilon_0$ ). In 0-10% centrality collisions,  $\varepsilon_0$  is large,  $\sim 20 GeV/fm^3$ . It decreases to  $\varepsilon_0 \sim 3GeV/fm^3$  in very peripheral collisions. Even in peripheral collisions, energy density is much larger than in cold nuclear matter ( $0.17GeV/fm^3$ ). We have also given prediction for high  $p_T$  suppression at LHC energy. For the same gluon density, high  $p_T$   $\pi^0$ 's are less suppressed at LHC energy than at RHIC energy.

---

\* e-mail:akc@veccal.ernet.in

- [1] J. Adams et al, STAR Collaboration, Phys.Rev.Lett.91, 2003,072304,nucl-ex/0306024. Phys.Rev.Lett.91, 2003,172302,nucl-ex/0305015. Phys.Rev.Lett.89, 2002,202301,nucl-ex/0206011.
- [2] S. S. Alder et al, PHENIX collaboration, Phys.Rev.C69,2004, 034910, nucl-ex/0308006. Phys.Rev.Lett.91,2003,072303, nucl-ex/0306021. Phys.Rev.Lett.91,2003,072301, nucl-ex/0304022
- [3] B. B. Back et al., PHOBOS collab. Phys.Rev.Lett.91,2003,072302, nucl-ex/0306025. Phys.Lett.B578 2004, 297.
- [4] I. Arsene, BRAHMS collab., Phys.Rev.Lett.91,2003, 072305.
- [5] M. Gyulassy and M. Plumer, Phys. Lett. B243, 1990, 432.
- [6] X. N. Wang and M. Gyulassy, Phys.Rev. Lett. 68 (1992) 1470.
- [7] J. C. Collins and D. E. Soper, Nucl. Phys. B194 (1982)445.
- [8] E. Wang and X. N. Wang, Phys. Rev. Lett.89,162301,2002 [arXiv:hep-ph/0202105].
- [9] X. N. Wang, nucl-th/0405017.
- [10] X. N. Wang, Nucl. Phys. A715, 775, 2003 [arXiv:hep-ph/0301196].
- [11] S. Y. Jeon, J. Jalilian-Marian and I. Sarcevic, Phys. Lett. B562, 45 (2003).
- [12] B. Muller, Phys. Rev. C67,061901, 2003 [arXiv:nucl-th/0208038].
- [13] I. Vitev and M. Gyulassy, Phys. Rev. Lett.89,252301,2002.
- [14] X. N. Wang, nucl-th/0305010.
- [15] I. Vitev, nucl-th/0404052.
- [16] K. Gallmeister, C. Greiner and Z. Xu, hep-ph/0212295.
- [17] A. Capella, E. G. Ferreira, A. B. Kaidalov and D. Sousa, inucl-th/0403081.
- [18] K. J. Eskola and H. Honkanen, Nucl.Phys.A713 (2003)167.
- [19] I. Sarcevic, S. D. Ellis and P. Carruthers, Phys. Rev. D 40(1989)1446.
- [20] B. A. Kniehl,G. Kramer and B. Poetter, Nucl. Phys. B582(2000)514.
- [21] A. Accardi and M. Gyulassy, Phys.Lett.B586,244,2004 [arXiv:nucl-th/0308029].
- [22] M. Gyulassy and X. N. Wang, Nucl. Phys.B420, 583(94) [arXiv:nucl-th/9306003]
- [23] R. Baier, Yuri L. Dokshitzer, Alfred H. Mueller, S. Peigne and D. Schiff, Nucl.Phys.B484,265,1997. [arXiv:hep-ph/9608322.]
- [24] R. Baier, D. Schiff, B.G. Zakharov, Ann.Rev.Nucl.Part.Sci.50,37,2000, [arXiv:hep-ph/0002198]
- [25] M. Gyulassy, P. Levai and I. Vitev, Phys. Rev. Lett. 85, 5535, 2000 [arXiv:nucl-th/0005032]; Nucl. Phys. B594, 371, 2001.
- [26] M. Gyulassy, I. Vitev and X.N. Wang, Phys. Rev. Lett.86,2507,2001. [arXiv:nucl-th/0012092].
- [27] U. A. Weidemann, Nucl. Phys. B588, 303, 2000.
- [28] X. F. Guo and X. N. Wang, Phys. Rev. Lett. 85,3591, 2000 [arXiv:hep-ph/0005044]; X. N. Wang and X. F. Guo, Nucl. Phys. A696, 788, 2001 [arXiv:hep-ph/0102230].
- [29] B. G. Zakharov,JETP Lett.73,49,2001 [arXiv:hep-ph/0012360].
- [30] J. D. Bjorken,FERMI-LAB-PUB-82-59-THY.
- [31] B. G. Zakharov, hep-ph/0410321.

## APPENDIX A: PATH LENGTH IN GLAUBER MODEL

The average length traversed by a parton at certain impact parameter can be obtained in the Glauber model. At impact parameter  $\mathbf{b}$ , the positions  $(\mathbf{s}, z)$  and  $(\mathbf{b} - \mathbf{s}, z')$  specifies the initial hard scattering of partons. The length traversed by the partons, after the initial hard scattering can be calculated as,

$$L(\mathbf{b}, \mathbf{s}, z, z') = \frac{1}{\rho_0} \left( \int_z^\infty dz_A \rho(\mathbf{s}, z_A) + \int_{z'}^\infty dz_B \rho(\mathbf{b} - \mathbf{s}, z_B) \right) \quad (\text{A1})$$

where  $\rho_0$  is the central density. Above expression should be averaged over all positions of initial hard scattering with a weight of the nuclear densities to obtain the path length at impact parameter  $\mathbf{b}$ .

$$L(\mathbf{b}) = \frac{\int d^2s \int dz \rho_A(s, z) \int dz' \rho_B(b - s, z') L(b, s, z, z')}{\int d^2s \int dz \rho_A(s, z) \int dz' \rho_B(b - s, z')} \quad (\text{A2})$$

TABLE I. For each centrality ranges of collisions we list the impact parameter ranges ( $b_{min}$  and  $b_{max}$ , Glauber model calculation of the average number of binary collisions ( $\langle N \rangle_{coll}$ ), and medium path length ( $\langle L \rangle$ ). Average transverse area ( $A_T$ ) calculated in a hard sphere model are also listed. Transverse gluon density ( $\frac{1}{A_T} \frac{dN_g}{dy}$ ) and gluon density ( $dN_g/dy$ ) in each centrality ranges of collisions are also shown.

centrality	$b_{min}(fm)$	$b_{max}(fm)$	$\langle N \rangle_{coll}$ ( $\langle N \rangle_{part}$ )	$\langle L \rangle$ (fm)	$A_T(fm^{-2})$	$\frac{1}{A_T} \frac{dN_g}{dy}(fm^{-2})$	$\frac{dN_g}{dy}$
0-10%	0.0	4.7	955.4(325.2)	5.174	102.2	$21.12 \pm 1.00$	$2158.3 \pm 102.1$
10-20%	4.7	6.7	602.6(234.6)	4.843	64.0	$16.94 \pm 0.89$	$1083.9 \pm 57.1$
20-30%	6.7	8.2	373.8(166.6)	4.396	43.9	$13.13 \pm 0.81$	$576.2 \pm 36.6$
30-40%	8.2	9.5	219.8(114.2)	4.014	28.7	$10.38 \pm 0.76$	$298.2 \pm 21.8$
40-50%	9.5	10.6	120.3(74.4)	3.393	17.3	$7.12 \pm 0.73$	$123.3 \pm 12.7$
50-60%	10.6	11.6	61.0(45.5)	3.032	8.7	$6.26 \pm 0.80$	$54.8 \pm 7.0$
60-70%	11.6	12.5	28.5(25.7)	2.276	2.9	$4.17 \pm 0.86$	$12.0 \pm 2.5$
70-80%	12.5	13.4	12.4(13.4)	1.450	< .65	$5.07 \pm 1.25$	< 3.3
70-92%	12.5	14.5	8.3(9.5)	1.164	< .65	$4.58 \pm 1.22$	< 3.0

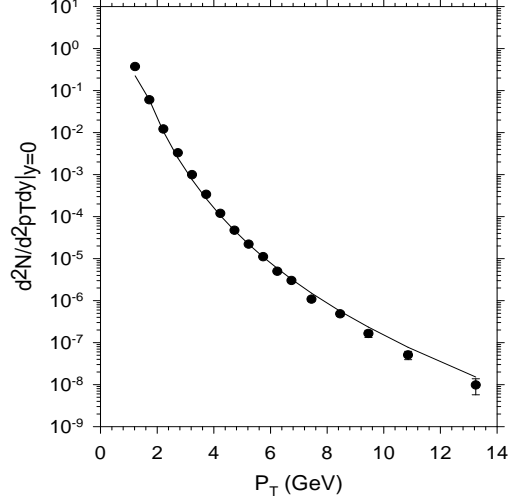


FIG. 1. The transverse momentum spectra for the neutral pions, in PHENIX pp collisions. The solid line is the pQCD model calculation.

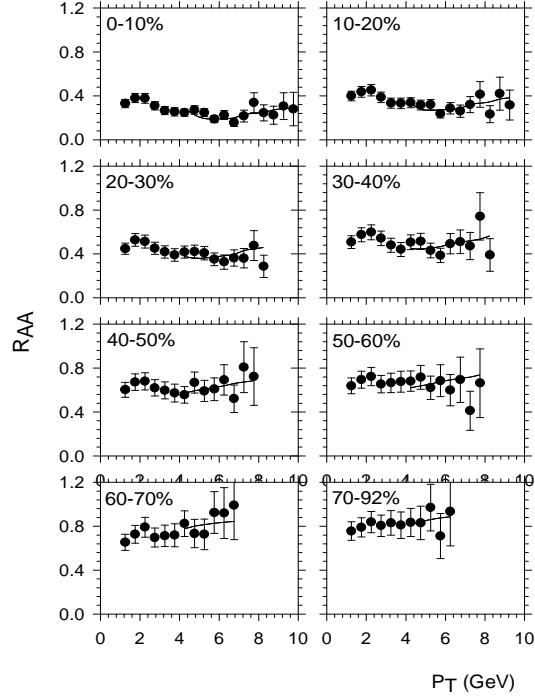


FIG. 2. The PHENIX data on nuclear modification factor for the neutral pions in different centrality of collisions. The solid lines are pQCD model fit to the data with jet quenching. Only free parameter is the initial gluon density.

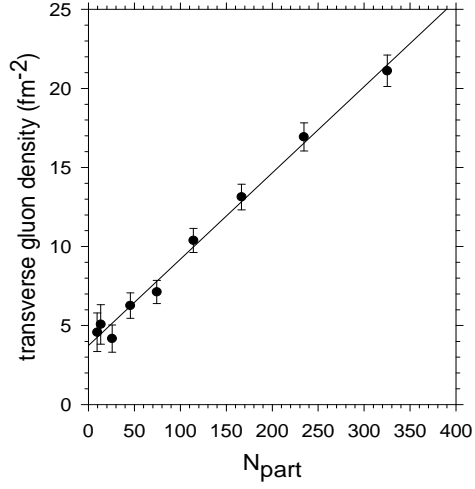


FIG. 3. Initial transverse gluon density ( $\frac{1}{A_T} \frac{dN_g}{dy}$ ) in different centrality ranges of collisions as a function of number of participants. Solid line is the linear relation,  $\frac{1}{A_T} \frac{dN_g}{dy} = 3.74 + 1.1 \frac{N_{part}}{2}$ .

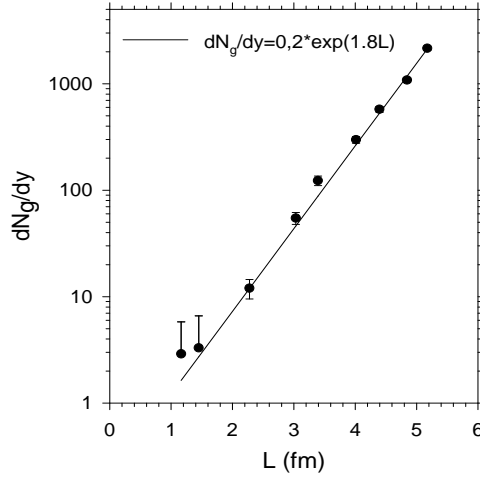


FIG. 4. Initial rapidity density ( $dN_g/dy$ ) of gluons, in different centrality of collisions are shown as a function of medium path length ( $L$ ). The solid line is a fit,  $dN_g/dy = 0.2 \exp(1.8L)$ .

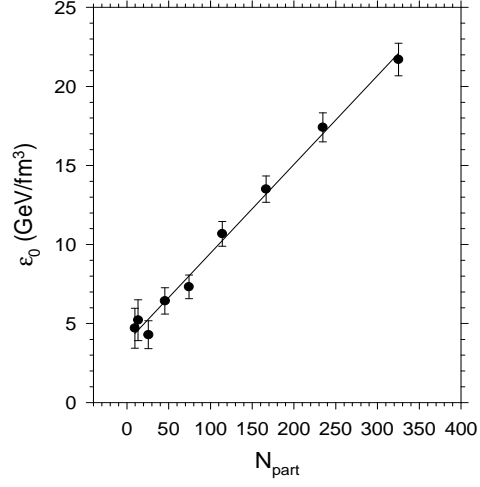


FIG. 5. Initial energy density ( $\epsilon_0$  in different centrality of collisions are shown as a function of participant numbers. The solid line is a linear fit to the energy density,  $\epsilon_0 = 3.84 + 1.1 \frac{N_{part}}{2}$ .

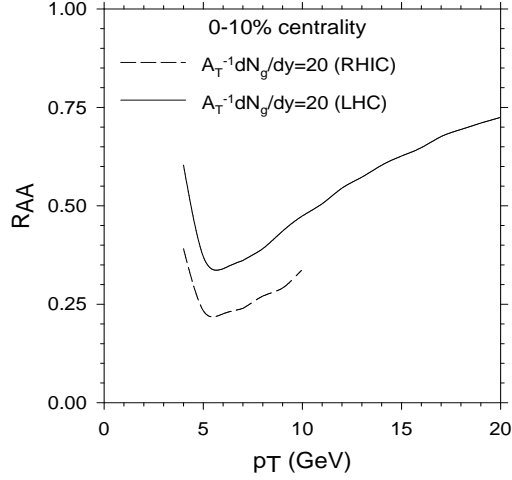


FIG. 6. Predicted nuclear modification factor in 0-10% centrality Au+Au collisions at LHC energy, shown as a function of transverse momentum. Initial transverse gluon density is  $\frac{1}{A_T} \frac{dN_g}{dy} = 20$ . For comparison, the same at RHIC energy is also shown (the dashed line).

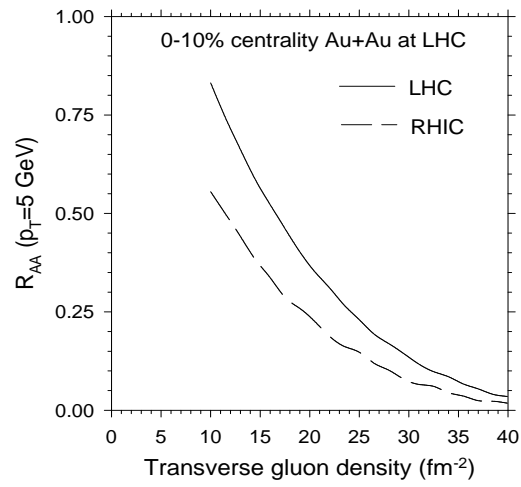


FIG. 7. Predicted nuclear modification factor at  $p_T=5$  GeV, in 0-10% centrality Au+Au collisions. The solid line and the dashed lines are for LHC and RHIC energy respectively.